JOURNAL OF MATERIALS SCIENCE 9 (1974) 81–99

Cyclic deformation and fracture of polymers

S. RABINOWITZ*, P. BEARDMORE
Metallurgy Department, Scientific Research Staff, Ford Motor Company, Dearborn, Michigan, USA

The cyclic stress-strain behaviour of a wide variety of rigid polymers has been studied. Three classes of fatigue response can be defined, each class displaying a characteristic evolutionary pattern in the stress-strain relation as deformation proceeds from the initial fatigue cycle to fatigue-crack propagation. Ductile polymers undergo a marked decrease in deformation resistance prior to crack formation; the detailed mechanism by which this "softening" develops can be related to the material microstructure and thermo-mechanical history. Amorphous polymers with a moderate degree of ductility soften slightly; in these materials crazing plays a dominant role in both the cyclic stress-strain response and the structural fatigue resistance. Brittle and nearly-brittle polymers are essentially stable in cyclic deformation; the fatigue resistance of these materials is very sensitive to strain amplitude in cyclic deformation.

1. Introduction

Polymers fail in fatigue. They do so, in analogy with more well-studied metals, because of a cycle by cycle accumulation of damage resulting from repeated non-elastic strain. Eventually, with a sufficient number of stress or strain applications above some limiting value (the so-called fatigue or endurance limit), a crack forms, propagates incrementally and the component (or laboratory specimen) fractures. Fatigue failure should, therefore, be a primary consideration in the development of polymers for load-bearing applications involving cyclic stresses. This requires information, only sparsely available at present, about the resistance of the polymer to cyclically induced fracture *and* about the stress-strain behaviour of the polymer under cyclic loading long before fracture.

Fatigue failure in polymers can be studied in several ways. From an engineering point of view, the fatigue life may be evaluated as a function of, say, the constant peak stress or strain, and the data displayed in the conventional stress versus log (life), (S-N) plot. This approach takes fatigue fracture as an event (rather than a process), and is of greatest utility in materials evaluation and selection for fatigue resistance. Most of the polymer fatigue research currently in the literature is of this type, and S-N data for various polymers and patterns of cyclic *stress* are available [1]. In recent years, an analytical technique for short-cutting the tedious experimental procedures involved in the generation of S-N curves has been developed in the study of the fatigue of metals [2-4]. In another paper [5], the fatigue resistance of a number of polymers in fully reversed uniaxial strain-controlled cycling will be reported within the framework of this technique.

It is emphasized that the S-N representation of fatigue resistance provides no direct information about the mechanism(s) of fatigue failure – that is, the mechanisms of fatigue-crack initiation or crack propagation. Comparison of the fatigue-life relations for a wide variety of polymers [5] indicates, however, that common patterns of fatigue behaviour exist, and some commonality in mechanism and response is implied. Taking the traditional "metallurgical" approach, the micro-mechanisms of cyclic deformation and fracture may be studied in individual polymer systems, or in systems grouped by type. This information is vital to the materials scientist if polymer microstructures are to be tailored specifically for fatigue applications. Some significant success in this regard has been attained, for

*Present address: Casting Division, Ford Motor Company, Detroit, Michigan 48239.

example, in designing the polypropylene "living hinge" [6]. Most of the other noteworthy efforts with respect to the mechanisms of failure have been directed towards the cyclic growth of fatigue cracks [7-9] – in fact, because of specimen transparency, one of the classic fatigue-crack propagation studies was carried out in a polymeric material [10]. On the other hand, little or no attention has been given to the mechanisms of cyclic deformation and fatigue crack initiation in rigid polymers. This is regrettable because fatigue fracture is initiation-controlled in all the homopolymers studied to date. In so far as such deformation studies depend on a thorough knowledge of the compliance modes in static or unidirectional loading, however, it is not surprising that there has been limited research on this topic; the molecular nature of yield and flow in glassy polymers is still only partially understood.

An alternative to the micro-mechanism approach to cyclic deformation and fracture is to consider the fatigue process phenomenologically, and to describe the cyclic behaviour in terms of the mechanics of deformation. This approach seeks to characterize fatigue failure parametrically on a macro level, i.e., in terms of the shape and slopes of the cyclic stress-strain relation, and gives only peripheral attention to the specifics of deformation in any one material. The phenomenology of cycle-dependent deformation in metals has been well characterized in recent years, and great success has been achieved in describing, predicting, and (ultimately) controlling fatigue failure in several alloy systems [2-4]. The same techniques have been used in the present work to define the cyclic stress-strain behaviour of a wide variety of thermoplastic polymers. As with metals, there are general patterns of cyclic deformation and fatigue resistance that are best defined in terms of the initial state of the polymer and the mechanics of response in monotonic deformation.* To establish these patterns of response, the detailed description of cyclic stress-strain behaviour given in this paper is sub-divided in terms of the different monotonic behavioural classes.

2. Experimental procedures

The strength-to-stiffness ratio for most engineering plastics is about one order of magnitude greater than for the common engineering metals. In strength-related service, therefore, the deflections developed in polymers are generally much greater than those developed in metals. Thus, it is most often the resistance of a polymer to repeated strains rather than repeated stresses that determines its fatigue behaviour in service.

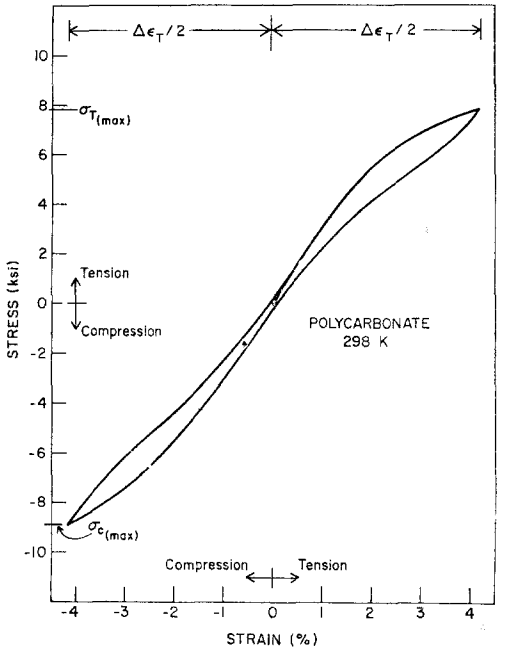

Figure 1 Initial hysteresis loop for PC cycled at 298 K, typical of *ductile* polymers. The definitions of various parameters used in the text are also indicated. 1 ksi = 10^3 psi.†

The experiments were executed in fully reversed (tension-compression), uniaxial strain-controlling cycling. With reference to the hysteresis loop for one complete cycle shown in Fig. 1, the strain range $\triangle\epsilon_T$ was maintained constant with equal elements $\triangle\epsilon_T/2$, in tension and compression. Note that only if the stress-strain relation remains constant during cycling is this test configuration equivalent to the more common stress-amplitude controlled fatigue testing. Because of the high mechanical damping and low thermal conductivity of most rigid polymers, considerable care must be exercised in cyclic deformation to avoid heat build-up in the specimen gauge length – it is possible to melt the sample in high strain, high frequency cycling

*The term "monotonic deformation" is used to denote unidirectional testing to yield or fracture; cyclic deformation involves at least one reversal in the sign of the strain-rate prior to fracture.
†10^3 psi = 6·89 Nmm^{-2}.

[11, 12]. The heating problem is often accentuated by the tendency for strain localization. To preclude a thermal contribution to this experiment, samples of poly(methylmethacrylate) and polycarbonate were instrumented with external and internal thermocouples, and the sample temperature was monitored during cycling at various strain-rates. It was found that at a strain-rate of 10^{-2} sec^{-1}, the temperature rise was less than 2°C prior to crack propagation in both materials; all tests were executed at this strain-rate.

All specimens were machined from commercially available 0.5 in. diameter rod stock. The uniform gauge length, 0.25 in. diameter and 0.30 in. long, was polished to a high brilliance using a mixture of stannic oxide and water. The details of the experimental arrangement have been reported elsewhere [13].

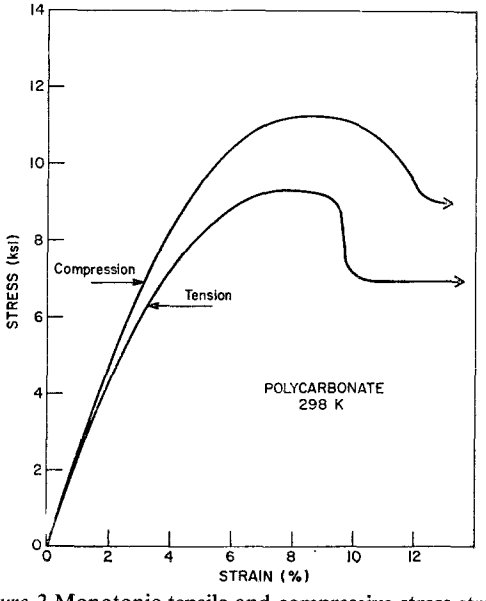

Figure 2 Monotonic tensile and compressive stress strain curves for PC at 298 K.

3. Results and discussion

3.1. Ductile polymers

The *ductile* polymer class is typified by polycarbonate deformed at moderate strain rates in air at room temperature, Fig. 2. *Ductile* polymers undergo large amounts of bulk flow in tension and compression. A sufficient criterion for membership in the *ductile* class is the manifestation of a discontinuous yield (as shown in Fig. 2), and this behaviour is typical of almost all *ductile* polymers; these include most semicrystalline homopolymers in the vicinity of room temperature, amorphous thermoplastics that do not (generally) craze, and amorphous thermoplastics in which crazes form but are ineffective as crack-nucleating defects. An example of the latter group is poly(methylmethacrylate) deformed in air at temperatures between about 40°C and the glass transition [14]. However, some *ductile* polymers (e.g., polyoxymethylene, glass-filled nylon 6/6) yield smoothly – the stress-strain relation maintains a positive slope – so the necessary conditions for *ductile* behaviour must be defined in terms of an as yet undetermined minimum strain to monotonic tensile fracture.

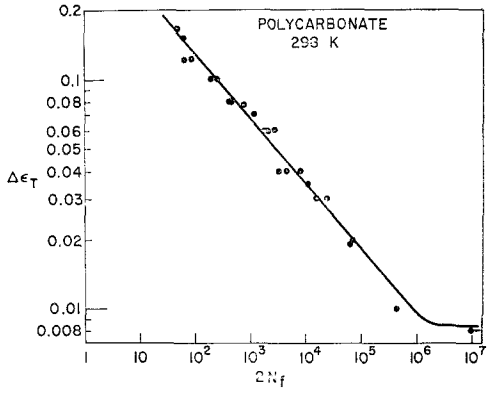

Figure 3 Total strain range versus reversals to failure for PC at 298 K.

Fig. 3 is a plot of the strain-life relation for polycarbonate at 298 K, represented as the logarithm of the total strain range ($\triangle\epsilon_T/2 + \triangle\epsilon_T/2 = \triangle\epsilon_T$ in Fig. 1) against the logarithm of the number of reversals (twice the number of cycles) to failure. The long range of linear proportionality (short and intermediate lives) is characteristic of *ductile* polymers, as is the manifestation of an apparent fatigue endurance limit at low strain levels. These fatigue data provide a convenient scaling reference for the discussion of the cyclic stress-strain behaviour of *ductile* polymers and are presented here for that purpose. Further consideration of fatigue longevity in polymers will be reserved for another report [5].

Fig. 1 shows the typical first cycle stress-strain response of a *ductile* polymer. The unusual propeller-like shape of the hysteresis loop is in marked contrast to the behaviour of metals where hysteresis loops roughly symmetric about the tip to tip axis are obtained (see, for example, Fig. 3 in [3]). The strain at any stress level can,

in theory, be separated into components deriving from elastic, anelastic and plastic processes. In a qualitative assessment, the deformation indicated by the first cycle hysteresis loop in Fig. 1 is predominantly elastic and anelastic, and the relaxation/recovery times characteristic of the deformation are on the order of the cycle time. The plastic strain per cycle is small; that is, the closure defect of the loop at zero stress is typically less than 2% of the strain range, and on the initial cycles recovery is almost complete if cycling is interrupted. The area enclosed by the hysteresis loop indicates the energy dissipated per cycle, $\triangle E$. For total strains greater than the fatigue endurance limit, the energy dissipation, expressed as a fraction of the total energy input per cycle – $Q^{-1} = \triangle E/E$ – increases with increasing strain to a maximum value of about 0.35 at about 8% strain (the upper yield point). At the other extreme, an extrapolation to low strain gives $Q^{-1} = 0$ at about the fatigue endurance limit, evidencing the strong correlation between energy dissipation and fatigue damage.

The peak compressive stress, $\sigma_{c(max)}$, is greater in magnitude than the peak tensile stress, $\sigma_{T(max)}$, for equal peak strains, $\triangle\epsilon_T/2$, Fig. 1. This flow strength differential (S-D effect) is characteristic of the uniform non-elastic deformation manifest in *ductile* and *semi-ductile* polymers (Section 3.2), and indicates the dependence of the deformation on the hydrostatic component of the applied stress [15]; the ratio σ_c/σ_T, taken in true stresses, gives a quantitative measure of the pressure dependence. This ratio is the same in monotonic deformation as it is in the initial cyclic response. After comparing other parameters of the stress-strain response, it is apparent that the initial cyclic behaviour is essentially identical to that obtained in monotonic deformation.

The most important feature of the initial cyclic stress-strain response of *ductile* polymers, however, is that it is unstable with respect to continued cycling; both the resistance to non-elastic deformation and the cyclic hysteresis undergo marked changes prior to fatigue crack initiation and propagation. The specific character of the changes in deformation behaviour induced by cycling depends on the test configuration (or service loading) – e.g., stress control or strain control – but the underlying deformation processes are the same. Thus, in cycling between equal stress limits in tension and compression (initially unequal strains because of the S-D effect), the changes in stress-strain response are in the nature of creep; on the other hand, cycling between equal strain limits (initially unequal stresses) induces changes in the nature of stress relaxation. Fig. 4 is an annotated reproduction of the experimental strip chart-recording of a strain-controlled fatigue test to failure in polycarbonate at 298 K. The lower half of the figure shows the imposed cyclic variation in strain at constant strain rate. The upper half of the figure is a continuous trace of the stress response to the imposed strain variation. The envelope of the stress trace indicates the cyclic evolution of the stress at peak strain in tension and compression. Four regimes of cyclic stress-strain behaviour can be discerned:

(1) an initial, or incubation, region in which the stress-strain response on the first cycle – the monotonic behaviour – is maintained practically unchanged;

(2) a transition stage, in which the peak stress decreases rapidly in tension *and* compression from one cycle to the next;

(3) a cyclic steady state region, in which the new stress-strain relation is maintained constant for a considerable number of cycles;

(4) a region of crack propagation terminated by fatigue fracture. In this stage the peak tensile load falls as the effective cross-sectional area decreases on each successive cycle, but the peak compressive stress remains essentially the same.

The cyclic stress-strain response of *ductile* polymers illustrated in Fig. 4, is termed *cyclic softening*. The transition from the monotonic stress-strain response to a cyclic steady state may be described phenomenologically as a decrease in material resistance to non-elastic strain with reversed deformation – a material softening. Phenomenologically, cyclic softening is not unique to *ductile* polymers, but is frequently obtained in cyclically deformed metals as well [2-4]. In fact, cyclic softening appears to be the general cyclic response of all discontinuously yielding* materials at strain levels below the

*Discontinuous yielding denotes the occurrence of a load drop in unidirectional straining. The load drop in most polymers occurs much more gradually than in, for example, what is generally taken as a true discontinuity in the stress-strain relation in bcc metals, but since it is difficult to separate the responses of specimen and test system at the upper yield point, and since the analogy with metallic behaviour is intended to be emphasized, the use of the term discontinuous is considered appropriate.

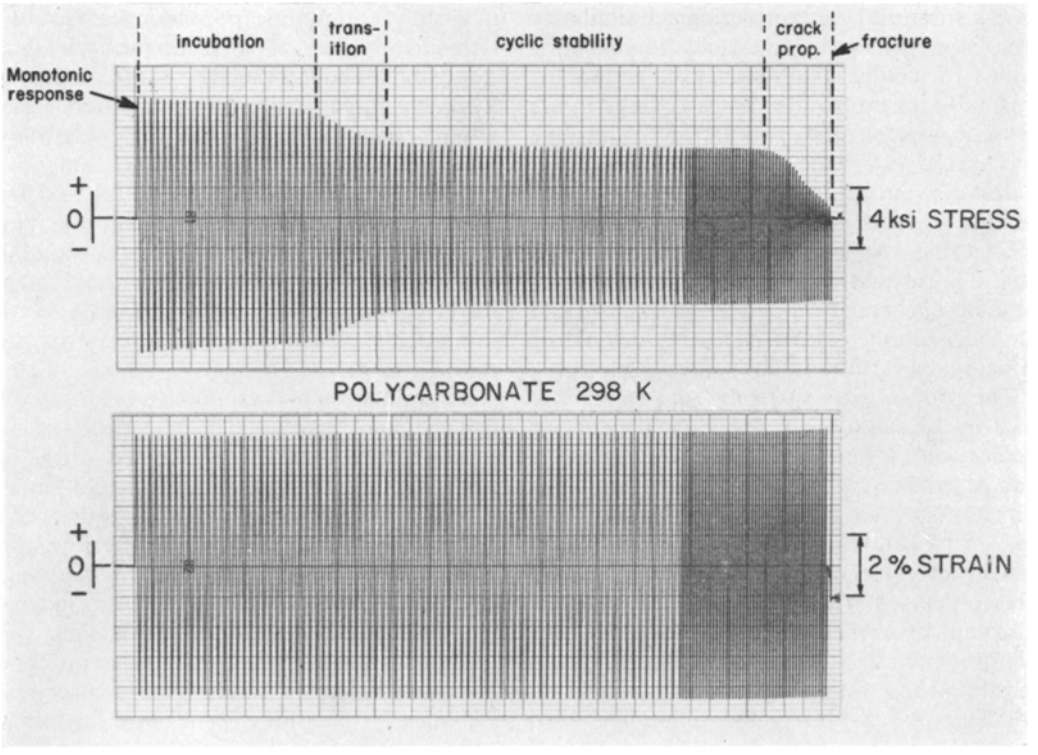

Figure 4 Reproduction of experimental strip chart recording for PC cycled in strain control at 298 K. The closer spacing of the cycles towards the end of the life is owing to a change in recorder chart speed.

upper yield strain. The converse, however, is not true; some materials (e.g., cold-worked copper [16], polyoxymethylene [5]) will cyclically soften even though their stress-strain relations exhibit a smooth, continuous yield. While it is not meant to imply that the micromechanisms of deformation in all discontinuously yielding (or cyclically softening) materials are the same, the similarity of phenomenological response is an important factor in understanding the fatigue behaviour of *ductile* plastics. In the following sections, the four regimes of cyclic response delineated in Fig. 4 will be discussed in relation to the overall fatigue life summarized in Fig. 3.

3.1.1. Incubation

The incubation period, as defined in Fig. 4, is a variable of both the initial state of the material and the imposed strain amplitude. At sufficiently high strain amplitudes, corresponding to fatigue lives on the order of 2×10^2 reversals or less for polycarbonate (Fig. 3), the sample begins to soften on the first cycle (see Fig. 6b), i.e., the incubation period is one reversal. As the imposed peak strain is decreased, the incubation period increases in duration and the amount of softening in the transition decreases. At sufficiently low peak strains, corresponding to fatigue lives on the order of 10^5 reversals and greater for polycarbonate, the incubation is longer than the fatigue life and the sample remains cyclically stable until a fatigue crack forms.

This sort of incubation period is not unique to cyclic deformation. In constant-stress (creep) experiments on discontinuously yielding metals and polymers, an incubation period of very low creep rate (delay time) is often encountered between the immediate elastic response and the onset of primary creep or neck formation. These similarities suggest that, phenomenologically, the deformation mechanisms can be described in an analogous manner (in creep and fatigue, in metals and polymers). The processes of large scale flow in *ductile* polymers likely involve the formation, growth, multiplication and motion of (some kind of) mobile defects, along the phenomenological lines of, but in no way

implying structural or morphological similarity to, the stress-activated multiplication of dislocations in metals. The incubation period (or delay time) then constitutes an early stage in the deformation when the population of mobile defects is too low to account for a significant non-elastic strain rate, but is increasing slowly. When the mobile defect population attains a critical value, softening (or primary creep) occurs. The formation of mobile defects takes place heterogeneously at adventitious sites of strain localization (caused by compositional or morphological variations, flaws, foreign particles, etc). The process is most likely auto-catalytic – at least in the sense of the Robertson theory of polymer yield [17], wherein the formation of one defect makes the formation of neighbouring defects easier – so that softening (or primary creep, or yield in monotonic deformation) occurs in an avalanche mode at the end of the incubation period. The rate of defect production and accumulation and, hence, the extent of the incubation period, varies with the state of the material and the test configuration.

For example, the integrated time-under-load prior to softening in fatigue is always less than the delay time in constant stress deformation at the same initial peak stress. Since the time at *peak* stress is only a small fraction of the total incubation period in the cyclic experiments, and since the rate of defect production is very stress sensitive, the localization of plastic strain that is promoted in reversed deformation must provide a potent driving force for defect production. Also, if a sufficient mobile population exists on (or immediately after) the first fatigue cycle, incubation is markedly reduced or even eliminated. Thus, as noted earlier, the incubation period is absent when polycarbonate is cycled above a threshold strain (or stress) level (cf. Fig. 6b); the production of mobile defects on the first tensile stroke satisfies the non-elastic strain-rate requirements for cyclic softening. It is also possible to envisage situations in which a material might go directly into the transition region at relatively low stress levels. If, by virtue of structure or thermomechanical history, a stable or steady-state population of defects exists prior to cycling, the required availability of adequate defect multiplication centres may be satisfied – cyclic softening then occurs immediately. In structurally inhomogeneous materials, regions of high local stress may exist at relatively low applied body stresses. Defect production in these regions can proceed at an accelerated rate, again pre-empting cyclic incubation. Both these effects likely contribute to the fatigue behaviour of such materials as nylon (and other semi-crystalline polymers), glass-fibre reinforced nylon (and other *ductile* fibre composites), and ABS (and other *ductile* rubber-modified thermoplastics); in all these materials, cyclic softening initiates on the first cycle and proceeds rapidly through the transition region at all strain levels at which softening is obtained. An example for nylon, typical of inhomogeneous microstructures, is shown in Fig. 5.

As a general rule, single phase, homogeneous

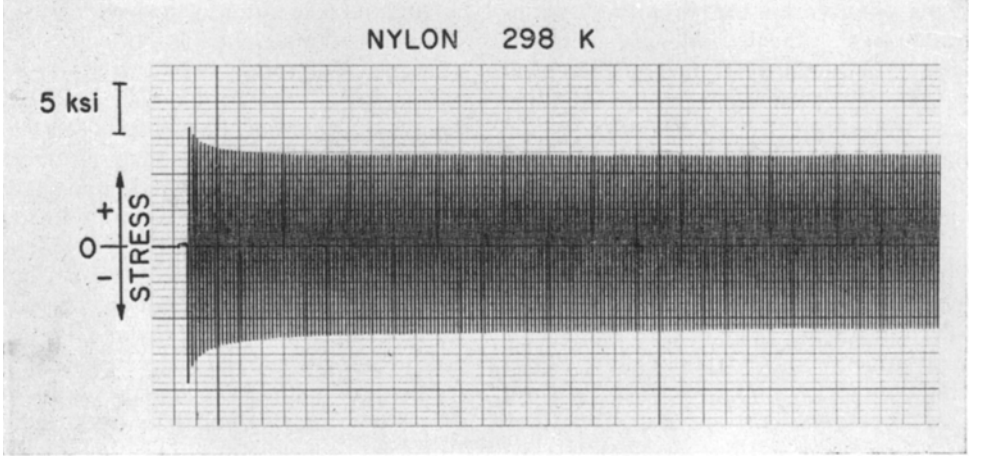

Figure 5 Reproduction of experimental record of the stress response of nylon in a strain controlled fatigue test at 298 K. Only the early part of the fatigue life is reproduced.

microstructures tend to exhibit a longer period of cyclic incubation in reversed deformation than do multi-phase microstructures. It is not meant to suggest that the character of the mobile defects, nor the mechanisms of their formation, multiplication, and interaction are similar within these material groupings; only the phenomenology of cyclic deformation is being described. It is possible, however, that studies of the kinetics of cyclic incubation can provide a means of characterizing, and perhaps identifying, specific defects and defect mechanisms in individual polymer systems.

In spite of the commonality of cyclic softening in all discontinuously yielding materials, it is interesting that the opposite effect, cyclic hardening, common in many metals displaying a variety of yield behaviours, is never obtained in polymers. Metals cyclically harden for the same basic reasons that they work harden in monotonic deformation – mobile defect-exhaustion, annihilation, mutual interference, etc. Work-hardening in polymers has not been studied simply because the molecular orientation hardening that invariably accompanies large scale bulk flow overwhelms and obscures any defect-hardening mechanism. However, the fact that polymers don't cyclically harden would indicate that such defect work hardening is small.

3.1.2. Transition

In the transition region, the stress-strain response changes rapidly; the peak stress decreases and the cyclic hysteresis increases from one cycle to the next. Fig. 6b shows the continuous stress-strain trace for a polycarbonate sample cycled at a relatively high strain amplitude – the specimen began to soften on the first cycle, and had a fatigue life of about 200 reversals to failure. It can be seen that from cycle to cycle the resistance to non-elastic deformation decreases and the cyclic energy dissipation increases in a continuous manner. Two important aspects of this softening process are noteworthy. First, there is no thermal contribution to the material softening; the transition region represents a true mechanical instability.* Second, softening proceeds approximately symmetrically in tension and compression – in other words, cyclic softening is not a manifestation of crack growth (cf. the behaviour in the crack propagation region in Fig. 4). In all *ductile* polymers, the transition region extends over only a few cycles, and constitutes a negligible fraction of the fatigue life. However, the changes that are induced in both mechanical response and molecular packing in the transition region have a profound effect on the fatigue resistance of *ductile* polymers; these phenomena are revealed in studies of the stress-strain behaviour of *ductile* polymers in the cyclic steady state.

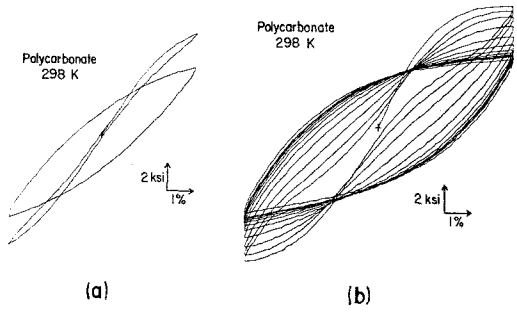

Figure 6 (a) Typical hysteresis loops for PC, showing the initial loop and a loop in the fully cyclically softened condition; (b) continuous trace of hysteresis loops for a PC specimen cycled between high strain limits showing continuous softening to steady state (heavy trace) condition.

3.1.3. Cyclic stability

In the fully softened condition, a *ductile* polymer maintains a new, steady-state stress-strain relation as cyclic deformation proceeds. The energy dissipated in driving the specimen through a complete cycle remains constant from one cycle to the next, and dynamic strain recovery processes balance the cyclically applied strain to give a constant cyclic non-elastic strain range.

Fig. 6 contrasts hysteresis loops obtained in the initial state and in the softened steady state for samples of polycarbonate tested at two different peak strain levels. Fig. 6a shows the first cycle, and a loop taken after attaining the steady state response, for a polycarbonate sample with a fatigue life of about 10^3 reversals. The high strain experiment illustrated in Fig. 6b has already been described – the sample began to soften on the first cycle and quickly established a cyclic steady state in which successive hysteresis loops superimposed to produce the heavy recorder trace.

*Thermal softening can occur in high strain and/or high strain-rate cycling, but the processes of heat generation and concomitant material softening are often runaway in a constant amplitude test; the specimen usually fails by melting or collapsing without ever attaining a cyclic steady-state response.

For a material with elastic and viscoelastic components to the total strain, the determination of the part of the total strain that is "damaging" in a fatigue situation is not straightforward. On any reckoning of fatigue damage, however, non-elastic strain and mechanical damping are the most important parameters [2]. To a first approximation, the maximum width of the cyclic hysteresis loop is an indication of the damaging strain per cycle, and the previously defined ratio $\triangle E/E = Q^{-1}$ indicates the normalized energy dissipation per cycle. The hysteresis loops in Fig. 6 dramatically illustrate that the fatigue damage per cycle is very much greater in the fully softened state than in the initial condition. For example, in the range of applied strains over which cyclic incubation is manifest in polycarbonate (fatigue lives on the order of 5×10^2 to 5×10^4 reversals), Q^{-1} increases about sixfold through the transition region (cf. Fig. 6a). At higher strains (no incubation), Q^{-1} increases only about 2 to 3 fold, as in Fig. 6b. The magnitude of the change in Q^{-1} is difficult to assess in the high strain region because softening begins on the first tensile half cycle. However, at the highest strains available in these experiments, approximately the tensile yield strain, the fatigue damage per cycle is still significantly greater than that in the initial state. In addition, for all *ductile* polymers tested, the largest fraction of the fatigue life is spent in the softened steady state. Thus, it is clearly the mechanical response of a *ductile* polymer in the cyclic steady state that ultimately controls fatigue failure. In fact, whenever changes in mechanical response are significant through the transition region, the monotonic stress-strain relation is a poor indication of fatigue resistance.

The most convenient and meaningful way to describe mechanical behaviour in the cyclic steady state is with a graphical representation of the steady-state stress-strain relation – this is termed the cyclic stress-strain curve [2, 3]. The applied peak strain and the steady-state peak tensile stress give, for example, one data point on the cyclic tensile stress-strain curve. By repeating the experiment in Fig. 4 at several strain levels, the entire cyclic stress-strain relation can be generated. In Fig. 7, the cyclic stress-strain curve for polycarbonate at room temperature is given, with the monotonic stress-strain relation included for comparison. Fig. 8 shows the similar response of a semi-crystalline polymer, nylon. In the initial region the cyclic and monotonic stress-strain relations are identical. Since the deformation in this low strain region is primarily elastic, the conclusion may be drawn that cyclic softening is a non-elastic strain process, involving primarily the anelastic and visco-plastic components of the strain. The amount of softening, i.e., the percentage stress difference between the monotonic and cyclic curves at constant strain, $\triangle\sigma/\sigma$, increases with increasing strain, to a maximum of about 40% at the upper yield point. These general comments are equally true in tension and compression, and a compressive cyclic stress-strain curve may be

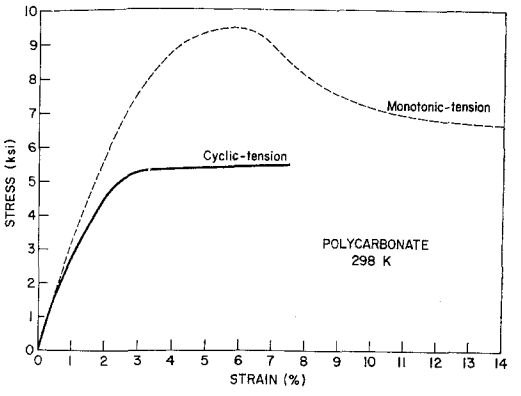

Figure 7 Tensile cyclic stress-strain curve for PC at 298 K. The monotonic curve is shown for comparison.

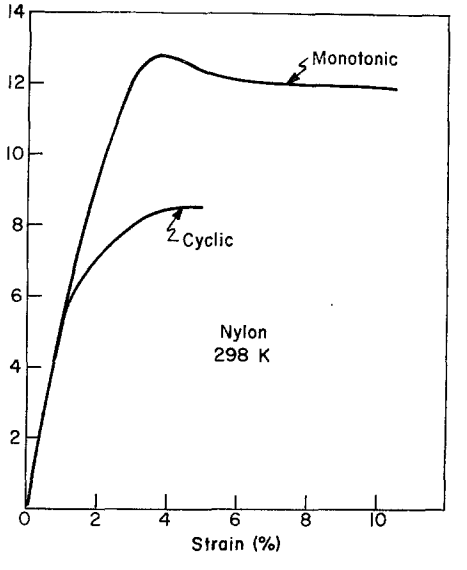

Figure 8 Tensile cyclic and monotonic stress-strain curves for nylon 6/6 at 298 K.

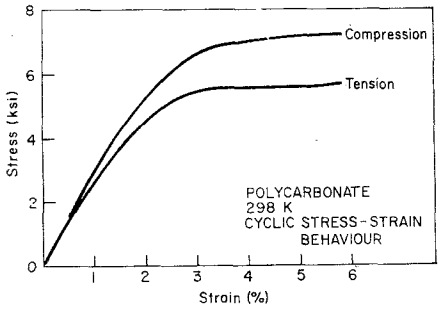

Figure 9 Tensile and compressive cyclic stress-strain curves for PC at 298 K.

defined analogously, Fig. 9. The magnitude of the strength differential between tensile and compressive flow stresses (S-D effect) manifest in the initial (pre-cycled) condition is approximately the same as is obtained in the cyclic steady state. Recalling that the S-D effect can be quantitatively related to the hydrostatic pressure coefficient of non-elastic flow in *ductile* polymers [15], this result (Fig. 9) supports the hypothesis that cyclic softening does not involve a change in the fundamental character of non-elastic deformation, but rather reflects a significant change in the relative rates of elastic and non-elastic strain processes, all of which are active throughout the fatigue life.

In the context of fatigue, the cyclic steady state is a dynamic condition; the large defect population and molecular rearrangement (see Fig. 10) produced in the softening process are sustained in the continuous deformation of the cyclic experiment. In a broader sense, however, the softened material can be considered a new material state, the properties of which can often be examined outside the fatigue situation that created it. For example, when a sample of PC is cycled into the steady state response and then removed from the test equipment after returning the stress on the sample to zero*, the new softened state persists indefinitely at room temperature. We designate this the softened *cyclic stable state*. Other *ductile* polymers that attain softened cyclic stability include nylon, polyoxymethylene, polysulphone and ABS. It must be emphasized, however, that cyclic softening and the attainment of a cyclic steady state do not imply such static stability. For example, *ductile* PMMA (above about 40°C and below T_g) manifests a softened steady state response during cycling, but recovers rapidly to the initial condition on removal from the fatigue test; the recovery is so rapid that attempts to quench PMMA to room temperature to preserve the softened state at zero applied stress have thus far proved unsuccessful. On a qualitative assessment based on the *ductile* polymers included in this study (all but PMMA tested at room temperature only), the attainment of cyclically *stable* behaviour depends on the location of the temperature range of *ductile* response relative to the temperature of strong molecular relaxation. In other words, independent of the fatigue considerations necessary to produce the softened state, stability depends on the rate of thermally activated recovery processes.

For a *ductile* polymer in the softened stable state, the cyclic stress-strain relation defined above indicates the general mechanical behaviour of the softened material. For example, if a softened specimen is removed from the fatigue apparatus and then retested in monotonic tension, the stress-strain relation thus obtained would trace the cyclic stress-strain curve. One obvious and important conclusion to be drawn from the results in Figs. 7 to 9 then, is that the yield discontinuity in monotonic deformation is eliminated in the cyclic stable state.† The discontinuous yield in monotonic deformation can be ascribed to the same phenomonological mechanism discussed with respect to the incubation and transition periods in cyclic deformation (Section 3.1.1) – an avalanche of mobile defects. By generating mobile defects in a relatively slow and homogeneous, cumulative manner in reverse deformation, the localized avalanche effect is obviated and a smooth, homogeneous transition into large-scale plastic flow results. In other words, the base-line mobile defect population in the softened state is stable – on reloading in monotonic tension, this population is already available for plastic flow. The large disparity in stress between the monotonic and cyclic stress-strain curves (Figs. 7 and 8) indicates that the

*With reference to Fig. 6, zero stress can be attained with either a tensile or compressive residual strain if the cyclic experiment is simply halted at the zero stress axis. However, by continuously decreasing the peak strain as cycling continues it is possible to drive the specimen back to the zero stress-zero strain origin; this procedure was adopted in all interrupted fatigue tests.

†Again, this phenomenon is not unique to *ductile* polymers. Discontinuously yielding bcc metals also exhibit a smooth yield in the cyclically stable state.

energy requirements for mobile defect generation (reflected only in monotonic curve) are much more severe than for defect motion (both curves).

It is interesting to point out the possible technological significance of this transition in material response during reversed deformation. Recent interest in the application of metal forming techniques (such as sheet stamping) to *ductile* polymers has highlighted the *ductile* polymer analogue to stretcher-strains in low carbon steel [18]. If polymers could be worked in the softened state, the problem of stretcher-strains might be eliminated; such cyclic pre-treatment (by flex-rolling) to metal stamping is already a viable process in discontinuously yielding metals [18].

The discussion of the mechanics of cyclic softening and the stress-strain properties of material in the stable softened state has been general to the *ductile* polymer class. Observations have been accumulated at room temperature on PC, nylon 6/6, nylon 6/6 with 13% glass fibres, ABS, polyoxymethylene and a partially cured epoxy, and on PMMA at 40 and 60°C. While the phenomenology of deformation is uniform within the *ductile* class, the specific mechanisms of plastic flow vary from one polymer to the next. For example, marked structural changes accompany cyclic softening in PC. Fig. 10 is a thin longitudinal section taken through the centre of a PC sample after cycling to the softened stable state condition. The softened material is clearly delineated as a region of marked molecular reorientation. Little dimensional change can be detected in the softened region on examination at low magnification – this is in marked contrast to neck formation in monotonic deformation. However, density measurements on softened PC indicate a 1% *increase* in density in the cyclic stable state. Similar observations have been made on softened samples of nylon 6/6. In nylon, the softened zone was delineated by a hardness trace along the specimen gauge length and by X-ray diffraction studies. The X-ray studies indicate a decrease in lattice *d*-spacing (compared to the initial material) and an increase in crystallite perfection for the softened material; again, softening produces an increase in material density.

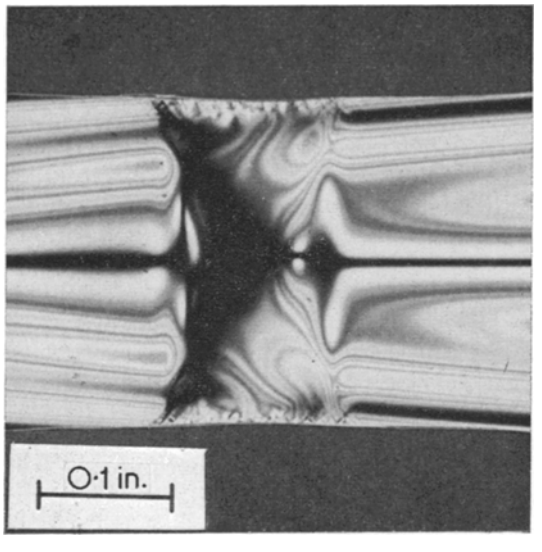

Figure 10 Thin section through softened region in PC.

Note that the densification of *ductile* polymers in cyclic deformation results in a decrease in resistance to non-elastic deformation. It is difficult to account for this behaviour on any free volume model of non-elastic deformation in rigid plastics. On the other hand, it is interesting to speculate on the possible correlation between these mechanical observations and the existence of ordered regions (presumably of higher density than the bulk sample) in amorphous thermoplastics [19, 20]. On the assumption that the ordered regions have a lower flow stress than the bulk polymer – resulting for example, from molecular packing efficiencies and a concomitant diminution in inter/intramolecular constraints (entanglements, configurational contortions, etc.) on large scale non-elastic flow – cyclic softening may reflect the stress-induced growth and coalescence of these regions. Whatever the mechanism, however, the softened stable state provides a unique material condition in which to study the process(es) of large scale non-elastic flow in *ductile* polymers. In conventional constant stress and constant strain-rate experiments, the transition into large flow is always accompanied by extreme strain localization (necking), and significant molecular orientation. The change in polymer properties with molecular orientation so overwhelms any other mechanical response, that observation of the underlying deformation mode may be totally obscured. In the softened stable state, a significant population of mobile "defects" can be established without gross molecular orientation; on redeformation of the softened material, the "defect" structure and properties are accessible for study.

Finally, with regard to attainment of a cyclically softened steady state, it should be pointed out the mode of cyclic control is important. In strain-limited tests (as discussed here), the transition to the softened state is always controlled and results in a steady state condition. However, in load control tests the transition may not be controlled depending on the peak stress level and specimen configuration. For example, at an initial stress level above the cyclic yield plateau (see Figs. 7 to 9), runaway creep failure would occur; at lower stress levels, a new steady state would be attained as defined by the same cyclic stress-strain curve obtained in strain control. In addition, as can be deduced from Figs. 2 and 9, asymmetric strain limits would result from equal load control limits, and the creep rate would be different in tension and compression. (Note that load control and stress control are not synonymous.) Thus, the mode of control can influence both the material response and the type of failure.

There is, perhaps, one final point to emphasize regarding the cyclic softening phenomenon. Irrespective of the particular defect mechanisms involved in the cyclic plastic deformation of *ductile* polymers, the phenomenological result is identical, overall cyclic softening. For example, crystalline defects (i.e., nylon), amorphous defects (PC) and crazing (ABS) are involved in the different polymers cited here, and yet these different yield mechanisms produce the same overall phenomenological result.

3.1.4. Crack propagation

The crack propagation stage of fatigue in *ductile* polymers is clearly evidenced in Fig. 4 by a cyclically decreasing peak tensile stress (caused by a cycle-by-cycle increase in crack area) and an approximately constant peak compressive stress. Such incremental crack growth is characteristic of (at least) the initial stages of fatigue crack propagation in *ductile* polymers, and is directly analogous to fatigue-crack growth in ductile metals [21].

Fig. 11 is a typical room temperature PC fatigue fracture surface – the sample was cycled at $\triangle\epsilon_T = 0.04$, and failed after $2N_f = 7000$ reversals (see Fig. 3). Fracture occurs in two stages. Over the area of the fracture surface ABCDA, true fatigue-crack growth has developed incrementally. An array of striae is clearly evident in this region. Each striation marks a site of crack arrest as the stress, driving

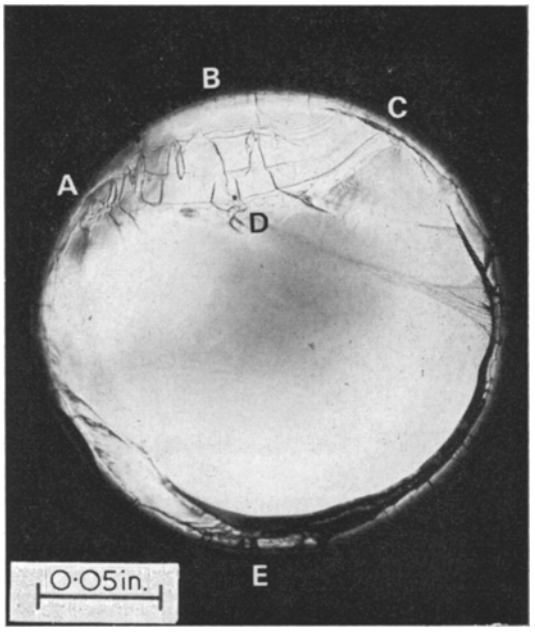

Figure 11 Typical fatigue fracture face in PC at 298 K, $2N_f = 7000$.

the crack forward, is reversed; the striae are formed via the crack-tip blunting/resharpening mechanism described by McEvily *et al* [10]. The distance between the striae increases as the crack front expands from its nucleus near point B in Fig. 11. The interstriation spacing (the crack growth increment) is proportional to the stress intensity at the crack tip. Thus, despite the cyclic decrease in load associated with crack propagation in a strain-controlled experiment (see Fig. 4), the increasing stress concentration factor associated with the growing crack keeps the stress intensity increasing until fracture.

When the crack attains a critical area, given by a modified Griffith criterion, catastrophic tensile fracture occurs over the remainder of the fracture surface, ADCEA. The extent of true fatigue-crack growth prior to catastrophic tensile failure increases with decreasing applied peak strain. Fig. 12 shows the effect in the fatigue failure of nylon at room temperature. The sample in Fig. 12a failed after $2N_f = 7500$ reversals at $\triangle\epsilon_T = 0.1$ (see Fig. 3); the region of true fatigue-crack growth is 23% of the total fracture surface. Fig. 12b is a corresponding fractograph for a sample cycled at $\triangle\epsilon_T = 0.05$ to $2N_f = 4.7 \times 10^5$ reversals to failure; at this lower peak strain, 55% of the fracture is fatigue-crack growth.

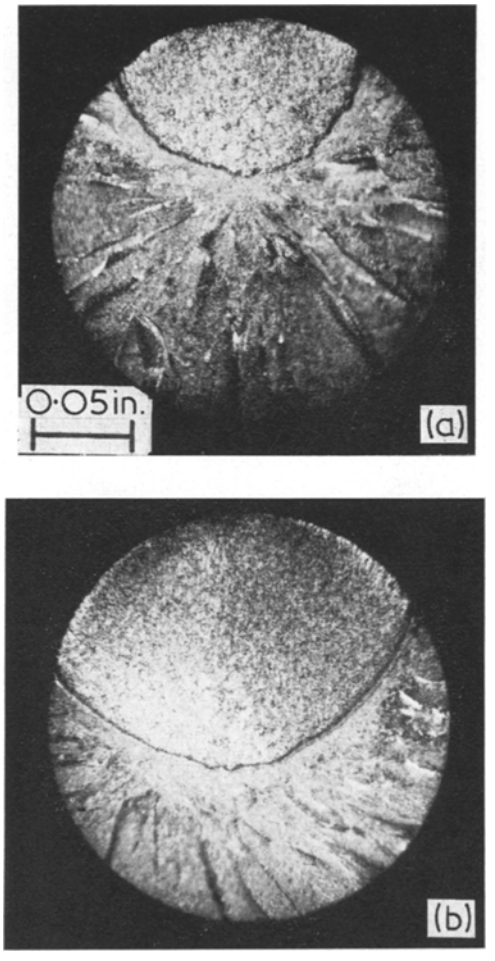

Figure 12 Fatigue fracture surfaces in nylon 6/6 showing increasing area of fatigue-crack growth with increasing life, (a) $2N_f = 7500$ reversals, (b) $2N_f = 4.7 \times 10^5$ reversals.

One important difference between the fatigue fracture surfaces in nylon and PC is that crack arrest striae are not resolved in nylon. The nylon macro stress-strain relation clearly indicates the incremental nature of fatigue-crack growth, but even at the shortest attainable fatigue lives the fatigue-crack growth rate is small compared to PC; thus, the cyclic growth increment may be too small to be resolved on the fracture surface. In addition, nylon fracture surfaces show a distinct pebbly texture, and the surface roughness may make resolution of fatigue striae impossible. The pebbly texture probably derives from some interaction between the growing crack and crystallite dispersion and orientation, but the exact mechanism of crack growth is currently not well established.

The incremental fatigue-crack growth described above occurs isothermally, i.e., there is no heating of the specimen up to the onset of catastrophic tensile fracture. However, a complication because of thermal effects can arise during fatigue-crack growth at high peak strains, even though the cyclic deformation prior to the development of a macroscopic crack was isothermal. The very localized nature of flow at the tip of the growing crack can result in significant heat generation at high peak strains, and a large temperature increase in the volume of material around the crack tip. Temperature increases of as much as 40°C have been measured during low-cycle fatigue-crack propagation in PC at ambient room temperature. When such heating occurs, the fracture mode changes. In particular, the high stress–high temperature condition at the crack tip enhances bulk plastic flow; the stress concentration at the crack tip is thereby reduced, the crack is "stabilized" and catastrophic tensile fracture is forestalled. With sufficient plastic flow at the crack tip, the fatigue crack can be made to propagate incrementally completely through the cross-section. An example of such a low cycle, high peak strain (large temperature increase during crack propagation) fatigue failure in PC at ambient room temperature is shown in Fig. 13. Fatigue fracture can be seen to proceed in an almost "controlled" manner, with the increment of crack growth on each cycle remaining fairly constant over much of the fracture surface. The amount of crack-tip heating and, hence, the fatigue crack stability, decreases with decreasing applied peak strain. For polycarbonate, the transition from non-isothermal to isothermal fatigue-crack propagation occurs at a fatigue life of about $2N_f = 1400$ reversals ($\triangle\epsilon_T = 0.06$).

It is emphasized that the isothermal fatigue fracture mode illustrated in Fig. 11 is a true fatigue fracture in PC, while that shown in Fig. 13 is only representative of fatigue-crack growth accompanied by significant specimen heating.

In contrast to PC, nylon shows no "thermal" transition in fatigue failure over the range of experimentally accessible peak strain amplitudes, Fig. 12. In this comparison, it is important to note that the non-elastic component of the total strain at the upper yield point (the limiting peak strain) is considerably smaller in nylon than it is in PC. Thus, the energy dissipated as heat on each tensile half-cycle is smaller in nylon, moving

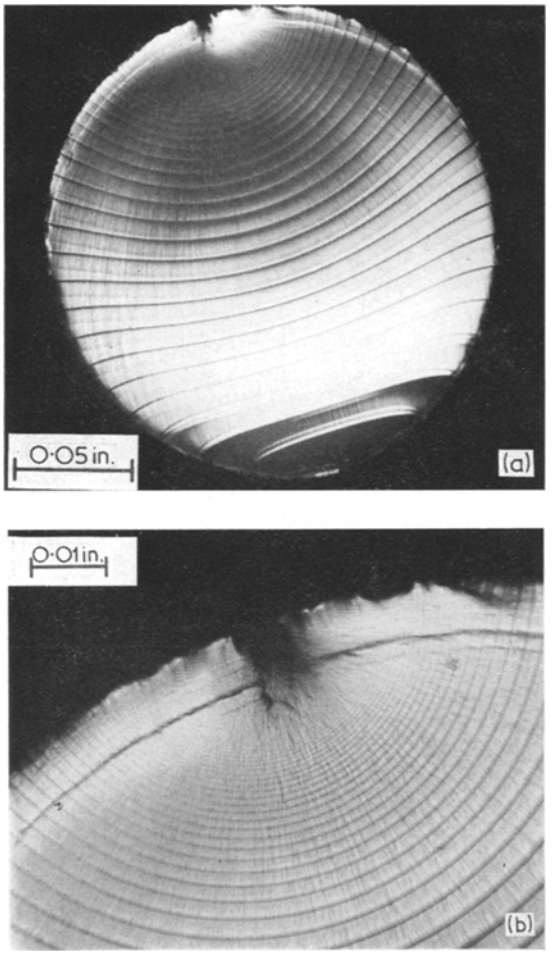

Figure 13 Typical fatigue fracture in PC when fatigue crack growth occurs with marked heating (a) overall fracture face, and (b) higher magnification of crack nucleus area showing the increasing interstriation spacing in the early stages of crack growth.

the "thermal" fatigue fracture transition to higher peak strains. In addition, the specific heat of the nylon is about 1.4 times that of PC, so the temperature rise per unit of mechanical energy released is smaller in nylon. If the high strain amplitudes corresponding to fatigue lives less than 10^3 reversals could be imposed in nylon, a "thermal" transition similar to that in PC probably would occur.

3.2. Semi-ductile polymers

3.2.1. General behaviour

The *semi-ductile* class of mechanical response is typified by poly(methylmethacrylate) deformed at room temperature, Fig. 14. In uniaxial

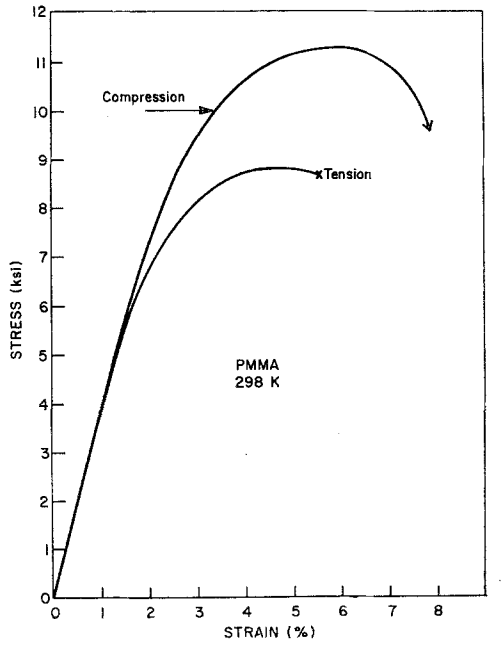

Figure 14 Monotonic tensile and compressive stress-strain curves for PMMA at 298 K.

compression, *semi-ductile* polymers undergo the same homogeneous flow processes operative in *ductile* polymers, and the two behavioural classes are indistinguishable. In uniaxial tensile deformation, however, the intrinsically ductile deformation response is accompanied by the simultaneous formation of potent crazes. The subsequent characteristic pattern of craze growth and craze breakdown to form a crack, pre-empts the continued development of the more homogeneous flow and the polymer fails prematurely [14]. Prior to fracture, however, the strain accommodated by this type of pre-emptive crazing is usually a negligibly small part of the total non-elastic strain [14, 22]; the shape of the monotonic stress-strain curve is determined by the same non-elastic compliance modes operative in *ductile* polymers.

Semi-ductile polymers are much more stable in cyclic deformation than *ductile* polymers. Fig. 15 is the typical *semi-ductile* stress response to strain controlled cycling; this PMMA sample was cycled at $\triangle\epsilon_T = 0.07$ (the upper yield strain is roughly 0.045), to $2N_f = 600$ reversals to failure.

A small amount of continuous softening occurs throughout the fatigue life, and a gradual decrease in both the tensile and compressive

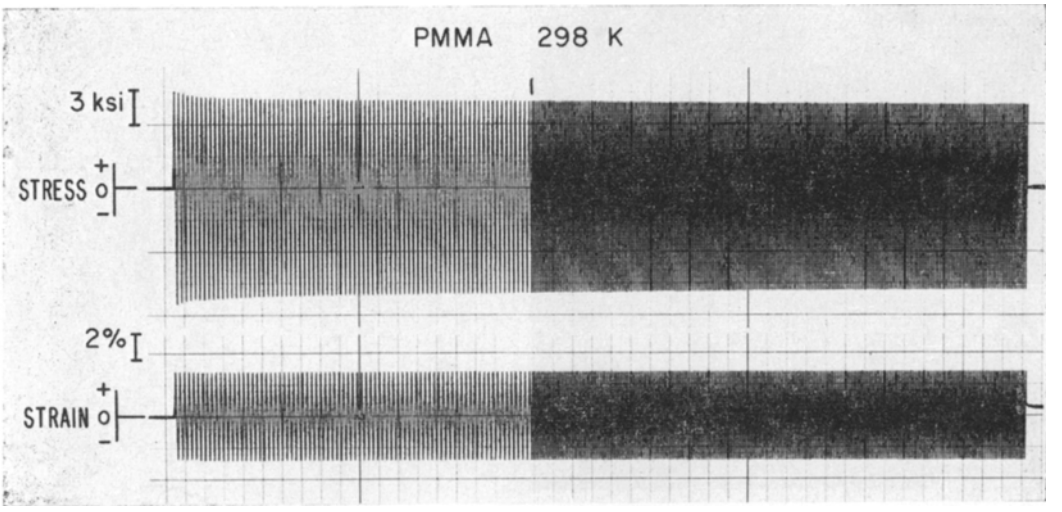

Figure 15 Reproduction of experimental strip chart recording for PMMA cycled in strain control at 298 K. The closer spacing of the cycles in the latter half of the fatigue life is owing to a reduction in recorder chart speed.

peak stresses is evident in Fig. 15. The total amount of softening is small relative to *ductile* polymers. At fracture the sample in Fig. 15 had softened about 13% in tension and compression; a PC sample at the same fatigue life softens almost 40%. Essentially, the entire fatigue life of *semi-ductile* polymers is spent in what has been defined as the incubation period in the previous section. Consistent with the small amount of cyclic softening, little change occurs in the hysteresis loops prior to fracture. For most of the fatigue life, the cyclic stress-strain relation is roughly coincident with the monotonic stress-strain relation.

Fatigue fracture occurs abruptly; no incremental fatigue-crack growth is indicated in the stress response in Fig. 15. Examination of *semi-ductile* fatigue fracture surfaces by visible-light microscopy reveals, however, a fracture mode qualitatively similar to that described for *ductile* polymers. Fig. 16 shows the fractur surface of a PMMA sample cycled at $\triangle\epsilon_T = 0.038$ ($2N_f = 3 \times 10^4$ reversals), as a typical representation of *semi-ductile* behaviour. There is no "thermal" transition in fatigue fracture in *semi-ductile* polymers, and Fig. 16 is qualitatively typical of fatigue fracture over the entire experimental fatigue life range.

The amount of true fatigue-crack growth prior to catastrophic tensile crack propagation is always small in *semi-ductile* polymers; in Fig. 16, for example, fatigue-crack propagation

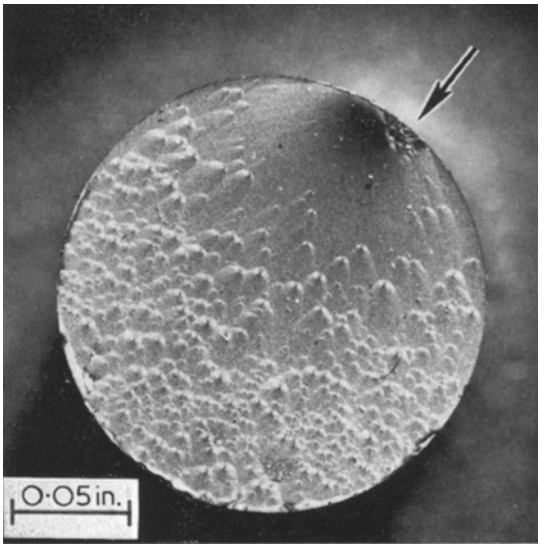

Figure 16 Typical fatigue-fracture face in PMMA at 298 K, $2N_f = 3 \times 10^4$ reversals. Arrow indicates crack nucleus region.

occurred over only about 25% of the apparent crack nucleus area, which itself comprises only 1.5% of the cross-sectional area. This can be seen in higher magnification images of the apparent nucleus region, as shown in Fig. 17a and b. In Fig. 17a the area of fatigue crack growth is designated ABCD; the larger fraction of the apparent nucleus region ADCEF was created by tensile fracture. Closer examination

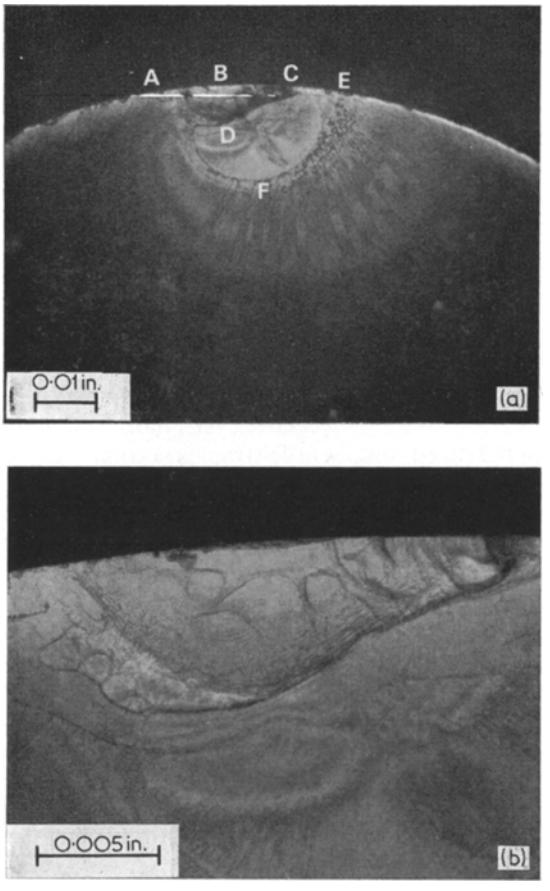

Figure 17 High magnification photographs of crack nucleus region in specimen shown in Fig. 16; (a) area ABCD outlines extent of incremental fatigue-crack growth, while area ADCEF is the first stage of the subsequent tensile fracture; (b) note the multiplicity of fatigue-crack origins within the overall fatigue-crack growth area.

of area ABCD, Fig. 17b, reveals that multiple fatigue-crack nuclei are formed, most likely as a result of the heterogeneous nature of craze breakdown (crack nucleation) in *semi-ductile* polymers [14], accentuated by the tendency to enhanced strain localization within the craze in cyclic deformation [23]. The individual fatigue cracks then merge to a common crack crack front prior to the transition to tensile failure. Moreover, within each crack nucleus, well-defined crack arrest striae are evident. As noted above, however, the incremental fatigue-crack growth responsible for the striae occurs over so small a fraction of the total cross-sectional area that no associated change in the macro stress-strain relation is detected in these experiments.

The tensile portion of fracture in the fatigue failure of *semi-ductile* polymers is identical to conventional monotonic tensile fracture – craze formation, craze growth, and breakdown of the craze structure [14]. The nucleation of a fatigue crack occurs in an analogous manner. Briefly, the tendency to strain localization in reversed straining promotes craze formation [23]. Continued cyclic deformation accelerates the formation of cavities and the coalescence of voids within the craze, and speeds the formation of a critical crack [23]. In the same sense as for monotonic tensile failure, crazes pre-empt the attainment in fatigue of the intrinsic ductility of *semi-ductile* polymers and induce a premature fracture.

It was emphasized in the definition of the *semi-ductile* class of behaviour that these polymers are intrinsically as ductile as their *ductile* counterparts. The question then arises as to why no pronounced cyclic softening occurs in *semi-ductile* polymers. As discussed in Section 3.1.1, cyclic softening is induced by an inhomogeneous deformation process involving the formation and growth of localized "pockets" of plastic strain. Crazing is a similar deformation process, and the scale of strain localization in the two is roughly the same. It is suggested that the dominance of the former compliance mode retards the development of macro softening – the crazes "soak up" the plastic strain necessary to induce softening; ultimately, increasing craze strain precludes cyclic softening by premature crack formation within a craze. It follows then, that if crazing is eliminated or rendered innocuous, the intrinsic ductility of *semi-ductile* polymers ought to be obtained, and gross cyclic softening should occur in fatigue.

3.2.2. Special behaviour

Crazing is a dilational deformation process requiring a critical level of principal tensile strain (or stress) to be attained locally [14], and for this reason crazes form preferentially at the free surfaces of the material. Thus, a particularly effective means of suppressing crazes is to induce a residual compressive stress in a thin surface layer by quenching the polymer rapidly to room temperature from above its glass transition [5]. If the layer of compressive stress is small, the stress-strain relation remains essentially unchanged with the exception that premature fracture is suppressed.

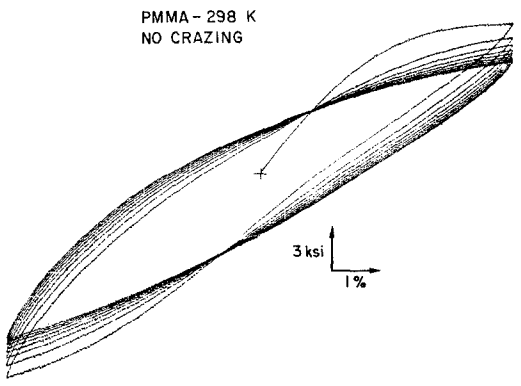

Figure 18 Hysteresis loops demonstrating the cyclic softening exhibited by PMMA at 298K when crazing is suppressed by thermal pre-stressing.

A sample of PMMA was thermally pre-stressed as described above. Fig. 18 shows the first several hysteresis loops when the sample was cycled to $\triangle\epsilon_T = 0.1$ at room temperature. When crazing is suppressed, PMMA behaves in a *ductile* manner at room temperature and exhibits macro cyclic softening. A similar softening can be induced in untreated PMMA by heating to about 40°C; at this temperature, crazes form but are relatively impotent as crack-nucleating defects [14].

One conclusion to be drawn from these observations is that cyclic softening is also surface nucleated. Apparently, the nucleation of softer regions in the sample interior is sufficiently difficult as to delay the process beyond the craze-breakdown event in normal *semi-ductile* response.

A different type of instability, manifest as a "tensile-only" softening, can occur in the cyclic stress-strain behaviour of *semi-ductile* polymers when craze growth proceeds to unusually large craze area prior to crack formation. Fig. 19 shows

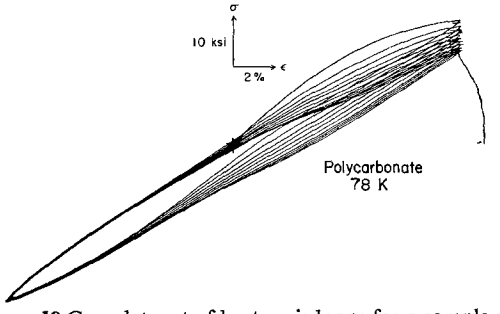

Figure 19 Complete set of hysteresis loops for a sample of PC tested at 77K in liquid nitrogen, 2 $N_f = 23$ reversals.

the complete set of hysteresis loops for a sample of PC tested at 77K, in liquid nitrogen, at $\triangle\epsilon_T = 0.22$ and $2N_f = 23$ reversals to failure. At this high peak tensile strain ($\epsilon = 0.11$) in cyclic deformation, PC crazes grow completely through the specimen cross-section prior to fracture in liquid nitrogen. The crazes actually grow incrementally on each tensile half-cycle in a manner described in detail elsewhere [23, 24].

On the initial cycle, the principal mode of strain accommodation is bulk flow in both tension and compression – note the large strength differential on the first cycle, characteristic of *ductile* type bulk flow. As craze area and craze thickness increase on each successive cycle, more and more of the (fixed) total tensile strain is accommodated in the crazes, at the expense of bulk flow. Since the crazes are more compliant than the uncrazed polymer [14], a progressive decrease in the resistance to tensile deformation occurs. On the compression half of each cycle there is no craze-strain contribution to the total applied strain, and the stress-strain relation remains unchanged. Note, however, that the point at which the current stress-strain relation merges to the initial cycle response shifts to ever increasing compressive stresses as deformation proceeds. This effect is probably caused by the increased difficulty of craze closure as craze thickness increases.

In many cases, confirmation of the incremental nature of craze growth, and the causal association with the stress-strain behaviour shown in Fig. 19, can be obtained directly from the fatigue fracture surface; an example is shown in Fig. 20. As discussed in detail elsewhere [24], the prominent concentric rings on the fracture surface mark the points of cyclic craze growth arrest as the craze grows inward from the surface in an annular ring configuration. There is a one-to-one correspondence between the number of rings and the number of cycles to failure in this low-cycle fatigue experiment.

Fatigue fracture occurs abruptly, as in other *semi-ductile* polymers; the sudden drop in load to zero is shown in Fig. 19. Crack nucleation within the craze proceeds in the conventional manner. However, with a large expanse of well-formed craze ahead of the crack as it begins to grow, the fatigue crack is channelled in the craze and a very smooth, planar fracture surface results. It is the smoothness of the surface that permits the sharp resolution of the craze arrest ring markings.

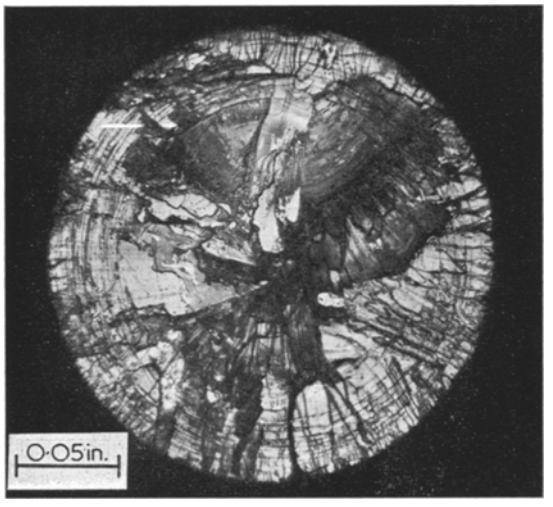

Figure 20 Typical fatigue fracture face in PC cycled at 77K. The concentric rings mark the lines of cyclic *craze* growth arrest.

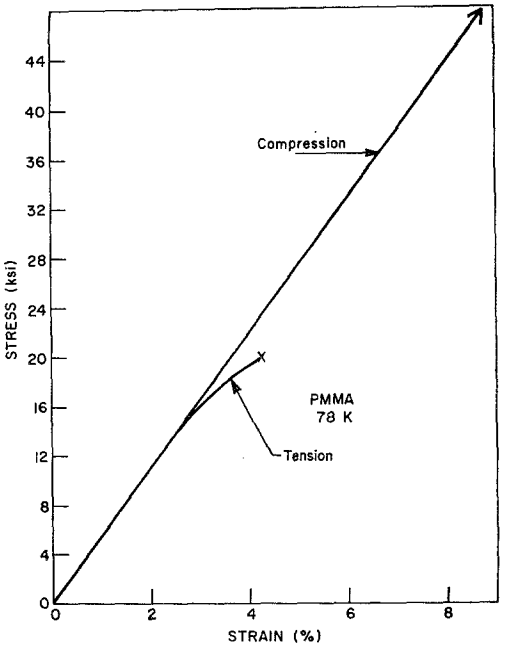

Figure 21 Monotonic tensile and compressive stress-strain curves for PMMA at 77K.

3.3. Semi-brittle polymers

The third class of monotonic stress-strain behaviour is the *semi-brittle* class, represented by PMMA deformed in liquid nitrogen at 77K, Fig. 21. For *semi-brittle* polymers the critical stress for homogeneous non-elastic deformation (the flow stress) is very much greater than the tensile fracture strength [25]. Thus, in the range of strains of interest in fully reversed cyclic deformation (from zero to plus and minus the tensile fracture strain) the bulk compliance is essentially elastic. The total non-elastic strain prior to fracture resides in large (area) thin crazes whose morphology differs quite distinctly from that obtained in the *semi-brittle* region [14, 26]. Since these crazes are the only source of non-elastic strain, and hence of fatigue damage, they are termed exclusive crazes to distinguish them from the pre-emptive crazes described above. For *semi-brittle* polymers, the stress-strain relation directly reflects the nucleation and growth of exclusive crazes.

Phenomenologically, *semi-brittle* polymers are stable in cyclic deformation. Because the total applied strain is primarily elastic, the fatigue life curve has a much lower slope than those for *ductile* and *semi-ductile* polymers at equal lives.

The only instability in the cyclic stress-strain response of *semi-brittle* polymers occurs at very short lives, when craze areal growth is extensive. As in the special case cited for semi-ductile polymers (PC at 77K), "tensile-only" softening can occur; however, because craze thickness development is retarded relative to craze areal development in *semi-brittle* polymers [14], the total craze strain is always small and the associated tensile "softening" is small. Indeed, in most cases the tensile stress decrease is insignificant.

The transition zones between the three classes of fatigue response are not always sharp; polymers tested within a transition region can display mixed fatigue response. A particularly good example, because its *semi-brittle* to *semi-ductile* transition zone falls in the vicinity of room temperature, is polystyrene. The fatigue behaviour of polystyrene has been described in detail elsewhere [23]; in brief, polystyrene behaves as a *semi-brittle* matrix polymer in which *semi-ductile* type (thick) large area crazes develop in fatigue.

At the extreme end of the *semi-brittle* behavioural domain are the truly brittle polymers – high cross-linked systems, highly-filled composites. Such systems have not been included in this study, but it is expected that their fatigue response is comparable to other brittle materials; namely, cyclic stability and a strong fatigue life strain sensitivity.

4. Mechanically anisotropic materials

The three classes of cyclic response discussed in this paper are appropriate to materials that are roughly isotropic in mechanical behaviour, and generally free of residual stresses. However, many polymers have commercial utility because of high molecular orientation and/or high residual stress and, the fact that such artificially introduced states of stress and molecular orientation are stable under static loading conditions (monotonic tension and compression, creep) does not guarantee that equal stability will be obtained in dynamic loading situations. Often, the cyclic stress-strain response of such mechanically anisotropic materials is unique, and it is difficult to generalize such materials as we have done with mechanically isotropic polymers.

One example of the unique type of cyclic response that can result from biasing the molecular orientation of a polymer is provided in the following experiment. A sample of polycarbonate was extended in uniaxial tension at room temperature until cold drawing was complete. The resulting specimen had a high degree of molecular orientation parallel to the tensile axis; on further deformation parallel to the orientation direction the compressive flow stress was about 0.65 of the tensile flow stress. The specimen was allowed to relax at zero stress for several days; then, the specimen was cycled, parallel to the orientation direction, between fully reversed strain limits.

Fig. 22 shows several hysteresis loops in the cyclic deformation – the first three cycles, and a cycle closer to the point of failure. A large reduction in the resistance to tensile deformation occurs (i.e. softening) whereas the compressive flow stress remains approximately constant. This is shown more clearly in Fig. 23, in which the peak tensile and compressive stress on each cycle is plotted against the accumulated cycles. The compressive peak stress remains essentially constant throughout the fatigue life. In marked contrast, the peak tensile stress decreases rapidly and continuously, to the approximate isotropic strength. This readjustment in deformation resistance occurs with no significant change in specimen birefringence, indicating that a high degree of molecular orientation is maintained. Presumably, the tensile softening results from residual stress relaxation and a possible intrinsic *ductile* softening; the compressive stress "stability" likely reflects a competition between intrinsic *ductile* softening and residual stress relaxation.

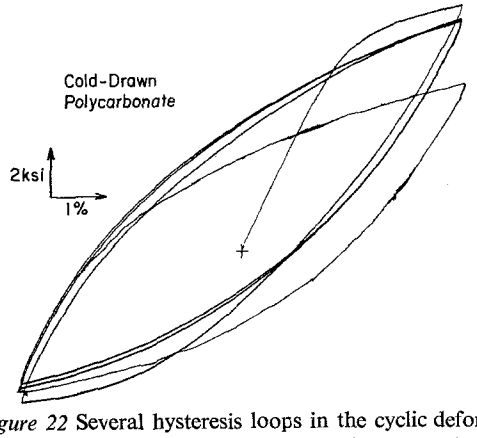

Figure 22 Several hysteresis loops in the cyclic deformation of oriented PC at 298 K – the initial three cycles and a cycle close to failure are shown.

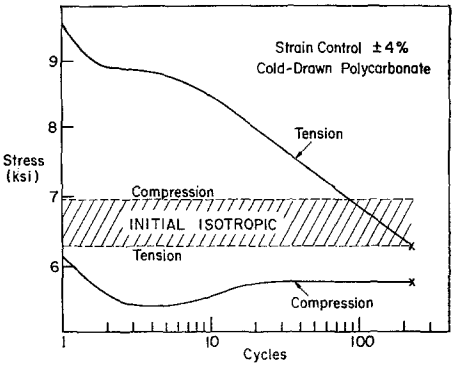

Figure 23 Peak tensile and compressive stress against accumulated cycles for the experiment shown in Fig. 22.

Note that cycling this sample has produced a unique structure/property combination – a highly oriented molecular structure, with little strength differential between tension and compression. The example cited above is used to illustrate the manner in which structural and/or internal stress variations in a material can produce unique cyclic responses. It is important to have some information about structural and mechanical isotropy of a material before conclusions regarding the origin of the cyclic response can be drawn.

5. Conclusions

It has been demonstrated in multiple examples that the cyclic stress-strain behaviour of rigid polymers, as with most metals, is not coincident

with the monotonic mechanical response. Thus, it is vital that the cyclic stress-strain behaviour be integral to the design for fatigue resistance in polymer components. In particular, because the cyclic response of any polymer component depends strongly on its thermomechanical history and ambient service environment, the specific cyclic response must be evaluated. However, the monotonic stress-strain relation in the service environment can serve as a guide to the general cyclic response and the phenomenological course of fatigue within the behavioural classes defined in this paper.

Acknowledgements

The authors are grateful to Dr R. Richman and Dr R. E. Robertson for helpful comment on the manuscript. Technical assistance in this study was ably provided by J. Ingall, T. A. Johnson and A. R. Krause.

References

1. G. F. CARTER (ed), "Fatigue and Impact Resistance of Plastics", Proc. of Fourth Annual Plastics Conf., Eastern Mich. Univ. (Industrial Education Department, 1969).
2. J. MORROW, *ASTM STP* **378** (1965) 45.
3. R. W. LANDGRAF, *ibid* **467** (1970) 3.
4. C. E. FELTNER and R. W. LANDGRAF, "Selecting Materials to Resist Low Cycle Fatigue", ASME Paper No. 69-DE-59 (1969).
5. P. BEARDMORE and S. RABINOWITZ, to be published.
6. R. D. HANNA, *Technical Papers, Soc. Plast. Eng.* **7** (1961) 16-3.
7. N. E. WATERS, *J. Mater. Sci.* **1** (1966) 354.
8. R. W. HERTZBERG, H. NORDBERG and J. A. MANSON, *ibid* **5** (1970) 521.
9. E. H. ANDREWS and B. J. WALKER, *Proc. Roy. Soc. Lond.* **A325** (1971) 57.
10. A. J. MCEVILY, R. C. BOETTNER and T. L. JOHNSTON, Tenth Sagamore Army Materials Research Conference (Syracuse University Press, 1964) p. 107.
11. M. N. RIDDELL, G. P. KOO and J. L. O'TOOLE, *Polymer Eng. Sci.* **6** (1966) 363.
12. I. CONSTABLE, J. G. WILLIAMS and D. J. BURNS, *J. Mech. Eng. Sci.* **12** (1970) 20.
13. C. E. FELTNER and M. R. MITCHELL, *ASTM STP* **465** (1969) 27.
14. S. RABINOWITZ and P. BEARDMORE, *Crit. Rev. Macro. Sci.* **1** (1972) 1.
15. R. A. DUCKETT, S. RABINOWITZ and I. M. WARD, *J. Mater. Sci.* **5** (1970) 909.
16. C. E. FELTNER and C. LAIRD, *Acta Metallurgica*, **15** (1967) 1621.
17. R. E. ROBERTSON, *J. Chem. Phys.* **44** (1966) 3950.
18. L. F. COFFIN, *Trans. ASM* **60** (1967) 160.
19. A. SIEGMANN and P. H. GEIL, *J. Macromol. Sci.* **B4** (1970) 557.
20. G. S. Y. YEH, *ibid* **B6** (3) (1972) 465.
21. C. LAIRD, *ASTM STP* **415** (1967) 131.
22. G. REHAGE and G. GOLDBACK, *Argew. Makromal. Chem.* **1** (1967) 125.
23. S. RABINOWITZ, A. R. KRAUSE and P. BEARDMORE, *J. Mater. Sci.* **8** (1973) 11.
24. P. BEARDMORE and S. RABINOWITZ, *ibid* **7** (1972) 720.
25. P. BEARDMORE, *Phil. Mag.* **19** (1969) 389.
26. P. BEARDMORE and S. RABINOWITZ, *J. Mater. Sci.* **6** (1971) 80.

Received 16 April and accepted 28 June 1973.